Proof of Concept of Kinematically Correct Neutrino Flavor Oscillations*

By **John Michael Williams**

jwill@AstraGate.net

EXT-2002-063

09/08/2002

* This posting provides details for a poster session of the same title, given Tuesday, 2002-08-13, at the Stanford Linear Accelerator Center: SSI 30th Summer Institute, *Secrets of the B Meson*.

Abstract

Assuming neutrinos have a flavor-independent and small but nonzero rest mass, flavor oscillations can be demonstrated which fit the known data without violating any physical law.

We require that the neutrino have observable substructure and an effective size, in at least one dimension, expanding after creation to exceed the range of the weak force. Thus, neutrinos are made truly analogous to kaons.

1. Assumptions

1. **Neutrinos can oscillate**, in the sense that they can change predominant flavor of interaction as a function of propagation distance (or, propagation proper time).

   Credibility: Recent experimental data at K2K, and observation at Super-K, SNO, and earlier facilities support this assumption, although a confirmed appearance experiment similar to that of LSND is required to close the door on alternatives.

2. **There are three flavors of neutrino**: electron, muon, and tauon.

   Credibility: Three flavors have been observed, and Z boson decay implies that no more than three light neutrinos can exist. Analogy with the Standard Model quarks and charged leptons suggests three flavors.

3. **The rest energy of all neutrinos is very small**. By small, we mean of the order of $mc^2 = 1$ eV or less.

   Credibility: Supernova and experimental data strongly support this assumption.

4. **Every neutrino is the source of a structured field which oscillates**. This field maintains an energy substructure or process of unspecified kind which evolves in proper time and causes flavor oscillation, when such is observed. Thus, the mass state and flavor state of a neutrino are quite unrelated.

   Credibility: Hypothetical. The assumption that such a field might be the cause of flavor oscillations is the primary basis for the new theory. Lepton substructure has been suggested by Calmet, et al [5].

5. **All neutrinos have the same nonzero expectancy of rest energy**. This is convenient but not necessary to our theory.

   Credibility: Hypothetical. Oscillations support this assumption by excluding mass hierarchy by flavor ([1], sect. 4.3; *cf.* [2]), but oscillations do not prove that initial interactions by flavor all yield the same rest energy.

2. General Constraints on Observability

To examine the observability of substructure internal to the neutrino, we initially take the spatial domain of any such substructure to be the range r of the weak force in the

rest frame of a freely propagating neutrino. We take $r \cong 10^{-17}$ m here, using the Compton wavelength of a W boson at rest as a somewhat arbitrary estimate.

In MKS units, then, from Heisenberg's principle, an observable internal momentum difference Δp then must be such that,

$$\Delta p \geq \frac{\hbar}{2\Delta x} \cong \frac{10^{-34}}{2 \cdot r} \Rightarrow \Delta p \geq 5 \cdot 10^{-16} \text{ kg} \cdot \text{m} \cdot \text{s}^{-1}. \tag{2.1}$$

Any change must propagate across a region this size in time Δt given by,

$$\Delta t \geq \frac{r}{c} \cong \frac{10^{-17}}{3 \cdot 10^{8}} \Rightarrow \Delta t \geq 3 \cdot 10^{-26} \text{ s}. \tag{2.2}$$

Consider a free particle which we would hope to use to probe spatial energy differences in a region with extent equal to r. For a massless particle, the energy associated with the momentum observable in (2.1) would be, $E = pc$; so, from (2.1),

$$\Delta E = \Delta pc \geq 1.5 \cdot 10^{-7} \text{ J} \Rightarrow \Delta E \geq 10^{12} \text{ eV}. \tag{2.3}$$

Hence, observation of a real, massless particle to measure spatial energy differences within a region known to be the range of the weak force is not possible for a neutrino interaction of less than about 1 TeV. For a massive particle of known rest energy ~10 eV $\cong 10^{-18}$ joule, which is a generous upper bound on the rest energy of the electron neutrino, the result in (2.3) is unaltered for any practical purpose. This result holds for collider experiments designed to probe substructure.

But, from Heisenberg's principle, in general,

$$\Delta E \geq \frac{\hbar}{2\Delta t}. \tag{2.4}$$

The time, and hence its uncertainty, may be arbitrarily large, for example, decay time of an unstable state, making a ΔE observable during that time arbitrarily small. So, **there is no essential lower limit on an observable change or difference in *E*** because of a process local to the particle of interest, provided the observation be made over an arbitrary time, long compared with the time in (2.2) in some specific frame of reference. This is the same argument as in the usual oscillation theories, the time being time in propagation.

Therefore, observation of an internal neutrino process based on spatial or other elements of arbitrarily small energy differences is allowable, provided the process not be sampled or observed over too short a time. The lower limit on the observation time-interval precision, Δt, may be estimated from (2.4).

3. Neutrino Wavefunction Representation

We wish to show that a generic wavefunction representation of flavor oscillation can support more than one theory of the mechanism causing the oscillation. This representation will serve as an outline for later development of the theory.

Consider the wavefunction Ψ_n of a neutrino as a product of three components,

$$\Psi_n = y_{\text{ position}} \cdot y_{\text{ flavor}} \cdot y_{\text{ spin}} . \tag{3.1}$$

We assume orbital spin to be irrelevant to freely propagating particles; isospin, C, P, T, etc. simply are ignored as irrelevant at present. Nothing in the present paper will distinguish neutrino from antineutrino; flavor and antiflavor will be assumed the same, in terms of oscillation. This approach is likely to be modified in later work.

To allow for three distinct flavor states, we must have, for a flavor-changing operator $\mathfrak{F}[]$, the unordered alternatives,

$$\mathfrak{F}[\Psi_n] \to \Psi_e , \ \mathfrak{F}[\Psi_n] \to \Psi_m , \ \mathfrak{F}[\Psi_n] \to \Psi_t . \tag{3.2}$$

These qualitative expressions are meant to represent nothing more than that the generic neutrino wavefunction, Ψ_n, must be able to interact at its annihilation as one or another of the three possible flavors.

Neutrino oscillations require the flavor probability at the point of final interaction to be a function of neutrino proper time in propagation; for the moment, we shall refer simply to the propagation distance, conventionally represented by the variable L. According to the usual theory of neutrino oscillations, with reasonably large mixing, for some three different (unordered) distances L_j from a specific neutrino creation point, we would require,

$$\mathfrak{F}[\Psi_n(L_1)] \to \Psi_e(L_1) , \ \mathfrak{F}[\Psi_n(L_2)] \to \Psi_m(L_2) , \ \mathfrak{F}[\Psi_n(L_3)] \to \Psi_t(L_3) . \tag{3.3}$$

The usual neutrino oscillation theories assume that only the position component in (3.1), used in a computation of a mass-eigenstate phase difference at distance L_j, defines the specific functionality of the operator $\mathfrak{F}[]$ in (3.3). In these theories, a neutrino is represented as a superposition of three wavefunctions as in (3.1), each one of a different, specific flavor. So, a propagating neutrino would have wavefunction representation in the flavor basis of the usual theory,

$$\Psi_n(L) = \left((y_{\text{ position}} \cdot y_{\ e})(L) + (y_{\text{ position}} \cdot y_{\ m})(L) + (y_{\text{ position}} \cdot y_{\ t})(L) \right) \cdot y_{\text{ spin}} . \tag{3.4}$$

In the usual theory, the $y_{\text{ position}}$ of the neutrino is derived from those of three alternative mass-eigenstate particles with independent kinematics. Mass eigenstates are postulated to differ slightly in rest energy; assuming this, the superposed phase indeed would vary secularly with L. This secularity would correspond to the length Δt of the time of observation of the previous Section. The superposed flavor state in (3.4) is obtained by

operation of a mixing matrix on the position-determined mass state. So, in the usual theory, final flavor depends critically on the three alternative position wavefunction phases.

However, equation (3.3) may be written from a different perspective as,

$$\mathfrak{F}_{L1}[\Psi_n] \rightarrow \Psi_e(L_1)\,,\ \mathfrak{F}_{L2}[\Psi_n] \rightarrow \Psi_m(L_2)\,,\ \mathfrak{F}_{L3}[\Psi_n] \rightarrow \Psi_t(L_3)\,. \tag{3.5}$$

Our initial assumption #4 above is intended to substitute the approach in (3.5) for the usual one in (3.3) or (3.4): We postulate an internal process which changes as a function of proper time (distance), defining the flavor change on the flavor component in (3.1). So, we assume that the position wavefunction component in (3.1) is not directly involved in neutrino oscillations. We question the assumption of the usual theory that the probability amplitude of the location in space of a neutrino interaction might determine the flavor of that interaction. By contrast with (3.4), our approach would be represented by,

$$\Psi_n(L) = \left(y_{\ e}(L) + y_{\ m}(L) + y_{\ t}(L)\right) \cdot y_{\ \text{position}} \cdot y_{\ \text{spin}}\,. \tag{3.6}$$

There is no special relationship of this representation with the Heisenberg picture methodology in quantum mechanics. Whereas the Heisenberg picture, contrasted with the Schroedinger or other picture, establishes a computational representation for a given problem, our approach in (3.6) means to postulate a mechanism different from that of Eq. (3.4), thus changing the physics of the problem.

We call the approach suggested by Eq. (3.6), ***internal oscillation***, because it depends on a process independent of the position wavefunction determining the amplitude of location of interaction of the neutrino with some other (external) particle or field. If we assume a unitary process, the internal oscillation will be equivalent to a flavor rotation over the distance L.

4. Physical Consistency of Internal Oscillation

We wish to verify that a unitary process representing the term in parentheses in (3.6), and explaining flavor oscillations, might be observable physically. We begin by computing the proper time of existence for what we would consider a typical neutrino; we then shall see whether this time is consistent with quantum mechanics as applied to unitary evolution of an extended object.

4.1. Relativistic Limits on Internal Oscillation

To relate proper time t_p of a freely propagating neutrino to lab frame time t and lab frame distance L, we need the total energy E and rest mass m of the neutrino in $E = mc^2 g$. The proper time t_p would be given by,

$$t_p = \frac{t}{g} \cong \frac{L}{c\,g}. \tag{4.1}$$

Let us assume the rest energy of the neutrino to be $mc^2 = 1$ eV. Then, for a 10 MeV Solar neutrino propagating $1.5 \cdot 10^{11}$ m from the core of the Sun to the Earth, we would have, from (4.1),

$$t_p = \frac{1.5 \cdot 10^{11}}{3 \cdot 10^8 \cdot (10 \cdot 10^6)} \cong 5 \cdot 10^{-5}\,\text{s}. \tag{4.2}$$

Similarly, for a 2 GeV atmospheric neutrino of the same rest energy propagating the approximate 10^7 m through the bulk of the Earth, we would have,

$$t_p = \frac{10^7}{3 \cdot 10^8 \cdot (2 \cdot 10^9)} \cong 2 \cdot 10^{-11}\,\text{s}. \tag{4.3}$$

In the LSND experiment, ~40 MeV (anti)neutrinos were allowed to propagate about 30 m; so,

$$t_p = \frac{30}{3 \cdot 10^8 \cdot (40 \cdot 10^6)} \cong 3 \cdot 10^{-15}\,\text{s}. \tag{4.4}$$

As expectable, for a neutrino of the same energy but lighter than 1 eV/c^2, the denominator in (4.2) – (4.4) would be larger, making the respective value of t_p smaller.

A unitary process is equivalent to a rotation. Given a massive point being orbitted in a circle with classical radius r equal to the range of the weak force, the cycle time t_c would be given by the tangential speed of rotation v_c as, $t_c = 2pr/v_c$. Relativistically, as we let $v_c \to c$, the effective mass of the particle will increase in the proper frame of the neutrino; to avoid this complication in preliminary calculations, we shall assume that the

speed does not become importantly relativistic, by restricting the domain to, say, $v_c < c/5$. We then have, for $r = r$,

$$t_c > \frac{10pr}{c} = \frac{10p \cdot 10^{-17}}{3 \cdot 10^8} \cong 10^{-24}\,\text{s}. \tag{4.5}$$

Tentatively, based on (4.4) and (4.5), we may require our internal oscillation process to be postulated with a cycle time t_c such that $10^{-24} < t_c < 10^{-5}$ seconds, implying an angular frequency w in the proper frame of the neutrino of about $10^6 < w < 10^{25}$. So far, this seems reasonable.

4.2. Quantal Limits on Internal Oscillation

First, we use Bohr's expression for quantization of angular momentum Q. For any extended object observed to rotate at angular frequency w, and for the rotational inertia I about the axis of rotation, we have,

$$Q = Iw = n\hbar \;\Rightarrow\; w = n\hbar/I\,. \tag{4.6}$$

This then imposes a quantal constraint on w for any geometrical unitary process. We use the word "geometrical" here to represent spatial variations of some kind in the energy in the weak field of a neutrino; the term refers only to amplitudes and expectancies, consistent with quantum mechanics. It is not meant to be different from any other way of describing a cyclic wavefunction phase shift.

In terms of cycle-time T_p in the proper frame of the rotating object, (4.6) may be written,

$$T_p = \frac{2pI}{n\hbar} \cong 10^{35}\frac{I}{n} \;\Rightarrow\; T_p \le 10^{35} I \,\text{seconds}. \tag{4.7}$$

To fulfill both the relativistic and quantal limits, we may eliminate duration between the inequality in (4.5) and the equality in (4.7) by setting $t_c = T_p$:

$$\frac{10pr}{c} \le 10^{35}\frac{I}{n} \;\Rightarrow\; r_p \le 10^{42}\frac{I_p}{n}, \tag{4.8}$$

in which the subscript p ("*p*roper") above and hereafter represents a value in the rest frame of the neutrino.

If a unitary process with observable geometric meaning is occurring during neutrino propagation, it must fulfill (4.8) in expectancy, by the principle of correspondence.

Second, we use Heisenberg's uncertainty principle to determine the imprecision in angular frequency we must allow to measure a well-defined phase angle in final interaction. The Heisenberg relation between phase angle and angular momentum Q is given by,

$$\Delta f \Delta Q \geq \frac{h}{4p}, \tag{4.9}$$

as discussed in [3].

To verify previous assumptions *ca.* Eq. (4.5) above, solving (4.8) for I_p we write,

$$I_p w_p \equiv Q_{\text{internal}} \geq 10^{-42} n r_p w_p . \tag{4.10}$$

The inequalities in (4.5), (4.8), and (4.10) represent a relativistic convenience, not a constraining uncertainty; we therefore define $\underline{Q}_p = \underline{I}_p w_p$ as the relativistic lower bound on Q_{internal} and apply Heisenberg's principle (4.9),

$$\Delta f_p \geq \frac{h}{4p\Delta \underline{Q}_p} = \frac{h}{4p \cdot 10^{-42} \Delta(\underline{n r_p} w_p)} . \tag{4.11}$$

In (4.11), let us denote by $\Delta \hat{w}_p$ a value of the Heisenberg Δw_p constrained by the relativistic lower limit $\underline{r_p}$. For example, now let $n = 1$, and, for $r_p = r = 10^{-17}$ m, let the Heisenberg $\Delta r_p = 10^{-18}$; with this, we would find the uncertainty in measured phase,

$$\Delta f_p \geq \frac{10^{-34}}{4p \cdot 10^{-42} 10^{-18} \Delta \hat{w}_p} \cong \frac{5 \cdot 10^{25}}{\Delta \hat{w}_p} . \tag{4.12}$$

So, to measure Δf_p to a usable precision, say 1 radian, we would have to have,

$$\Delta \hat{w}_p \geq 5 \cdot 10^{25} \text{ s}^{-1}, \tag{4.13}$$

which barely meets the constraint of (4.5) and at first glance might seem not to permit much flavor oscillation variation by distance or energy in the (4.2) – (4.4) typical neutrino cases.

However, $\Delta \hat{w}_p$ in (4.13) depends on the postulated small value of Δr_p. There is no reason relativistically or quantum-mechanically why Δr_p could not be as large as, say, 10^{-10} m, about the size of an atom perhaps involved in a neutrino interaction. With this change, then, from (4.11), instead of (4.13), we would have,

$$\Delta \hat{w}_p \geq 5 \cdot 10^{17} \text{ s}^{-1} . \tag{4.14}$$

A recalculated Eq. (4.5) would be,

$$t_c > \frac{10 p r_p}{c} = \frac{10p \cdot 10^{-10}}{3 \cdot 10^8} \cong 10^{-17} \text{ s} \Rightarrow w_p \cong 10^{18} \text{ s}^{-1}, \tag{4.15}$$

which necessarily is consistent with the new uncertainty constraint in (4.14).

Returning to (4.11) and going to the extreme indicated by the typical neutrino parameters above, if we took $\Delta r_p \cong 10\,\mathrm{m}$, we would have $\Delta \hat{w}_p \cong 5 \cdot 10^6\ \mathrm{s}^{-1}$, within range of an average frequency adequate to explain the Solar neutrino problem. Even for the relatively low-energy Solar neutrino in (4.2), it should be noted that the Lorentz-contracted length r of the internal structure would be at most about $10^{-6}\,\mathrm{m}$ in the lab frame.

Thus, it appears possible to postulate internal oscillations by increasing r_p greatly beyond the range of the weak force. This implies an extended size for the neutrino particle, as has been suggested for other reasons in [2]. We shall return to this issue later, when deciding how to model the neutrino in a consistency check preceding actual theory development.

4.3. Internal Oscillation Should Not Contribute To Spin

The neutrino is believed to be a fermion with intrinsic spin of $\pm 1/2$. If the internal oscillation process is to represent rotation of a massive structure, the oscillation will be associated with an angular momentum Q, and each quantum of Q in principle would add to the intrinsic spin angular momentum s of the neutrino to give its total observed angular momentum.

We are assuming that the neutrino is not elementary; so, we might allow it, like a fermionic atom, to have angular momentum of $s + Q$. However, such a condition would make calculation of the properties of the particle more complex than seems necessary.

We therefore require, consistent with the factoring away of spin in Eq. (3.6), that the internal oscillation not affect the angular momentum of the neutrino. Two possible ways to achieve this would be:

(*a*) to assign the angular momentum of internal oscillation to the imaginary axis, making the rule of addition, for n quanta, something like,

$$Q_{\text{neutrino}} = s + n \cdot iQ_{\text{internal}} \Rightarrow \mathrm{Re}(Q_{\text{neutrino}}) \equiv s\ ; \text{ or,} \tag{4.16}$$

(*b*) to define the internal oscillation as that of a structure with counter-rotating components of opposite momentum, so that the internal motion would be governed by the Q of each component, but that the total contribution would be cancelled:

$$Q_{\text{neutrino}} = s + n \cdot (Q_+ + Q_-) = s + n \cdot 0 \equiv s\,. \tag{4.17}$$

The first alternative (4.16) has obscure implications; so, for the present purpose, which merely is a consistency check, we shall adopt the second, counterrotating alternative given in Eq. (4.17). We shall assume exactly two such components.

We still need a rationale to use the counterrotation to calculate the internal oscillation frequency. There would seem to be several qualitatively different approaches:

(*a*) Only one phase might be assumed involved in flavor oscillation and the second ignored. Thus, phase of the internal oscillation would be determined with respect to

some direction in the rest frame of the neutrino--for example, the direction of neutrino propagation.

To model this assumption in the simplest way, we would divide the internal structure equally between rotation and counterrotation: This would imply that only half of the mass in the internal structure would contribute to the rotational inertia I determining oscillation frequency, the other half merely would cancel the internal angular momentum.

(*b*) Both of the counterrotating phases might be used to define the flavor oscillation. The predominant flavor at any moment in neutrino proper time would be given by coincidence of two phases, one of rotation and one of counterrotation, and other spatial features in the rest frame of the neutrino could be ignored. Again assuming equal division of the mass, this would imply a flavor oscillation frequency twice that of either phase--which is to say, twice that calculated under the previous approach (*a*).

(*c*) An evolution might cause the counterrotating structures to vary secularly in the potential of the weak field of the neutrino, a secular function of one or both phases defining the predominant flavor at final interaction. Here, one might imagine adapting the CKM or PMNS matrix derivation to internal oscillations to calculate flavor; however, we shall leave that possibility for others, or for a later paper.

At present, we take the first, simplest approach: We shall calculate the value of Q_{internal} based on a rotation of half of the available mass, the other half being dedicated to cancellation of the angular momentum caused by the internal oscillation process, whatever might be its nature.

4.4. Internal Oscillation Radius of the Neutrino

Naively, let us now look at the value of rotational inertia implied by what we believe known of the neutrino:

We already have assumed *ca.* Eq. (4.5) that I will be taken as applying only to nonrelativistic rotary motion. For a sphere of uniform density and radius r, the classical rotational inertia is given by $I = (2/5)mr^2$. For a negligibly thin rod of length r, $I = (1/12)mr^2$. The maximum possible centric value would be $I = mr^2$, for the mass concentrated in a thin ring or cylinder at distance r from the rotational axis.

Keeping in mind the huge sizes required by the Heisenberg constraint above, we decide to preserve a spatially point-like interaction for the neutrino by assuming it to be elongated only in the direction of propagation. So, as a try, we accept a thin rod model. Because of the counterrotation assumption of (4.17), the mass will be halved, leaving us with an expression for ***the rotational inertia of internal oscillation***,

$$I = mr^2/24 . \tag{4.18}$$

Substituting this for I_p in (4.8), we get a radius (assumed not 0) in the rest frame of the neutrino of length,

$$r_p \le 10^{42} \frac{m r_p^2}{24n} \Rightarrow r_p \ge 2.4 \cdot 10^{-41} \frac{n}{m}. \tag{4.19}$$

Assuming a neutrino rest mass of 1 $\text{eV}/c^2 = 1.6 \cdot 10^{-19}$ kg, from (4.19) we may obtain a lower limit on the size of the neutrino internal structure,

$$r_p \ge 1.5 \cdot 10^{-22} n \text{ meters}, \tag{4.20}$$

which clearly is consistent with the sizes required above. It is not obvious that a meaningful lower limit on the neutrino mass might be obtained from (4.19), because of the large values of r_p required for realistic neutrino oscillations *ca.* Eq. (4.15).

The preceding calculations assumed the entire rest energy of the neutrino to be allocated to the structure representing the unitary, flavor-changing process. If the actual process associated with flavor oscillations involved less than the total rest energy, then the value in Eq. (4.20) would be increased to fit a limit based only on the fraction of the rest energy associated with the flavor-changing process.

5. A Tentative Quirk Theory of Internal Oscillation

At this point, we adopt [2] the term, *quirk structure*, to refer to an energy substructure of the neutrino, with features called *quirks*, which defines a rotation (unitary process). We refine the initial assumptions above thus:

Quirk Assumption 1: The quirk structure maps to the unitarity of neutrino oscillations.

We do not suggest that quirks can be isolated or examined as though particles; nor do we suggest that the energy of a quirk can be changed. The postulation of quirk structure merely is another way of describing something with a linear size that might have phase features of some kind, making rotation meaningful. We do allow energy to be stored in the quirk structure as a whole, and to be exchanged with energy in the weak (or other local) field during propagation. However, rest energy of the neutrino is not allowed to change.

Quirk Assumption 2: Flavor amplitude is determined by the quirk phase.

As the quirk structure rotates in proper time of propagation, each flavor in turn dominates the neutrino final interaction cross-section.

Given three flavors of neutrino, we assume initially that each flavor will map to a specific $2p/3$ of each quirk cycle. For any initial flavor, there will be two other flavors possible. So, neutrino experiments sensitive to flavor, expecting the same flavor in initial and final interaction, and observing oscillations, typically will show a disappearance; this is no different from the usual oscillation theory.

The suggested dependence on proper time implies an inverse dependence of oscillation frequency on energy, at a given distance between initial and final neutrino interactions; this is in the same direction as in the usual oscillation theory (e. g., Eq. (2.17) in [2]).

Quirk Assumption 3: The quirk radius expands after neutrino creation.

To explain the wide range of propagation distances over which oscillation seems to occur, we suggest that when a neutrino is created, the radius (linear size) of the quirk structure is minimal; as the neutrino propagates, this radius increases. This implies that exact unitarity of the flavor-changing process will not be observed secularly, at least during the earliest times in propagation, although energy will be assumed conserved within the neutrino as a whole. Thus, oscillation frequency will be higher near the neutrino creation point than at great distances. The relatively short range LSND and K2K results seem to argue for some such expansion.

6. Empirical Consistency of the Quirk Theory

We now apply the quirk assumptions to some data to clarify the idea and to test consistency of the theory in an artificial and very simple context. We use Table 6.1 below to collect limits on parameters of a workable neutrino model.

Because LSND has reported apparent oscillation from muon flavor into (anti)electron flavor, we tentatively accept this to define a global direction of quirk phase such that the flavor rotation is in the direction, $m \to e \to t \to m \ldots$. The result is shown in Fig. 6.1 below. It would be possible to define the initial direction of rotation, as well as the initial phase (flavor), as somehow dependent on parameters such as energy, parity, or other quantum numbers of the initial particle(s), or even perhaps by a probability amplitude derived somehow from the initial interaction; however, at present we prefer simplicity to universality.

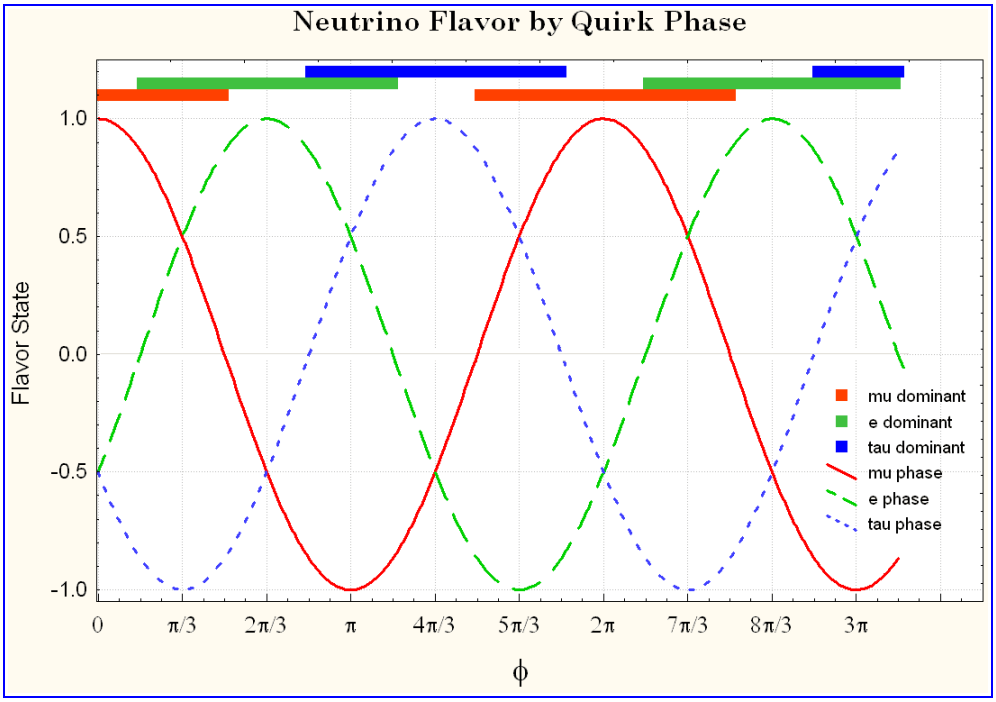

Figure 6.1. Flavor variation scheme consistent with Quirk Assumption #2. Regions of dominance are indicated by the horizontal bars at top.

In Fig. 6.1, we show one possible interpretation of Quirk Assumption #2 in Section 5, above. In this figure, the separate amplitudes of the three flavors are plotted as functions of quirk phase during propagation. We ignore the imaginary part for the present purpose. Each color-coded horizontal bar near the top of the figure indicates the domain on which the respective flavor state was positive. The bars are offset vertically slightly for clarity. This representation of "dominant" flavor is for graphical purposes only, to illustrate the sequence of dominant flavors as defined above and in Table 6.1.

We next estimate the minimum quirk phase f for the three proper times in (4.2) - (4.4) likely to account for the LSND, atmospheric, and Solar neutrino effects, respectively; these are entered in Table 6.1. The known experimental discrepancies (~0.05 : ~0.4 : ~0.4) respectively are fit coarsely by a guess at the quirk phase assumed to cause it. The cycle count is just the number of full flavor oscillation cycles in the value of f assumed (with no attempt at precision) to explain the three example data.

A few routine calculations are recorded above the blue box in Table 6.1. After that, using the estimated phase f, the quirk structure angular speed w_p is calculated over the propagation distance as,

$$w_p = \frac{f}{T_p}, \tag{6.1}$$

which also is entered in the table. If r_p is not assumed fixed, but would change with propagation distance, then Eq. (6.1) would make $w_p = < w_p >$ an average.

Table 6.1 A coarse data fit by internal oscillation theory. Quantities subscripted *p* (*p*roper) are in the neutrino rest frame.

$m \to e \to t \to m$	Example Data Set		
Parameter	Experimental	Atmospheric	Solar
Neutrino mass m	$1\,\mathrm{eV}/c^2$	$1\,\mathrm{eV}/c^2$	$1\,\mathrm{eV}/c^2$
Neutrino energy E	40 MeV	2 GeV	10 MeV
Neutrino Lorentz g	$4\cdot10^{7}$	$2\cdot10^{9}$	$1\cdot10^{7}$
Neutrino Compton l_C	$3\cdot10^{-14}\,\mathrm{m}$	$6\cdot10^{-16}\,\mathrm{m}$	$1.2\cdot10^{-13}\,\mathrm{m}$
Propagation Distance L	$3\cdot10^{1}\,\mathrm{m}$	$10^{7}\,\mathrm{m}$	$1.5\cdot10^{11}\,\mathrm{m}$
Proper time T_p	$3\cdot10^{-15}\,\mathrm{s}$	$2\cdot10^{-11}\,\mathrm{s}$	$5\cdot10^{-5}\,\mathrm{s}$
Flavor change	$m \to e$	$m \to e \to t$	$e^2 \to t$
Quirk cycle count	0	0	1
Quirk phase f	$p/2\,0$	$2p - p/2 = 3p/2$	$2p + p/2 = 5p/2$
Quirk angular mom. n	1	1	1
Quirk w_p	$5\cdot10^{13}\ s^{-1}$	$2.4\cdot10^{11}\ s^{-1}$	$1.6\cdot10^{5}\ s^{-1}$
Quirk w	$1.3\cdot10^{6}\ s^{-1}$	$10^{2}\ s^{-1}$	$1.6\cdot10^{-2}\ s^{-1}$
Quirk radius r_p	$1.8\cdot10^{-14}\,\mathrm{m}$	$2.6\cdot10^{-13}\,\mathrm{m}$	$3.2\cdot10^{-10}\,\mathrm{m}$
Quirk radius r	$3\cdot10^{-22}\,\mathrm{m}$	$8\cdot10^{-23}\,\mathrm{m}$	$2\cdot10^{-17}\,\mathrm{m}$
Rotary energy K	$1.7\cdot10^{-2}\,\mathrm{eV}$	$8\cdot10^{-5}\,\mathrm{eV}$	$5\cdot10^{-11}\,\mathrm{eV}$

Using $I = m r^2/24$ from Eq. (4.18) and $Iw = n\hbar$ from Eq. (4.6), we may write in general,

$$r_p = \sqrt{\frac{12hn}{pmw_p}} \;\Leftrightarrow\; w_p = \frac{12hn}{pr_p^2 m}. \tag{6.2a}$$

Using this and assuming that the quirk structure holds just $n = 1$ quantum of angular momentum, we may describe the quirk radius of a generic $1\ \mathrm{eV}/c^2$ neutrino by,

$$r_p \cong 1.3\cdot10^{-7} w_p^{\,-1/2}\ \text{meters}; \tag{6.2b}$$

which is in eV units and equivalent to the formula for frequency,

$$w_p \cong 1.7\cdot10^{-14} r_p^{-2}\ \mathrm{s}^{-1}. \tag{6.2c}$$

The values of lab-frame r are computed from r_p on the assumption that Lorentz contraction would be the circular average in the direction of neutrino propagation, or,

$$r = \frac{2r_p}{p\,g}\,\mathrm{m}. \tag{6.3}$$

Also, we estimate the (potential) energy change in the weak field because of the postulated change in quirk structure radius r; this energy would be the difference between an arbitrary constant and the rotary kinetic energy K of the quirk structure. Nonrelativistically, we know $K = I w_p^2/2$. Using the previous assumption that $I \cong m r^2/24$, the table displays the resulting values of,

$$K = \frac{m r_p^2 w_p^2}{48}\,\mathrm{eV}, \tag{6.4}$$

for m in eV/c^2.

To verify that our data values of w_p and r_p in Table 6.1 can fit previous quantum assumptions, we next estimate the Heisenberg uncertainty Δf in quirk phase, given a reasonable uncertainty in quirk frequency w_p as defined on the right in Eq. (6.2a):

Both (6.2) and (6.3) may be interpreted as representing point expectancies or measured values. A specific measurement in final interaction will have Heisenberg uncertainty dependent on the uncertainty in angular momentum Q as given by Eq. (4.9) above. Using (4.18),

$$Q_{\mathrm{internal}} = I w_p = \frac{1}{24} m r_p^2 w_p\,. \tag{6.5}$$

Then, from (4.9), taking r_p and $m \equiv 1\ \mathrm{eV}/c^2$ as unobserved parameters,

$$\Delta f \geq \frac{12h}{\Delta w_p p \cdot 1.6 \cdot 10^{-19} r_p^2}; \tag{6.6a}$$

or, approximately, setting a reasonable criterion of 1 radian for Δf,

$$r_p \geq 5 \cdot 10^{-8} (\Delta w_p)^{-1/2} \;\Leftrightarrow\; \Delta w_p \geq 5 \cdot 10^{-8} r_p^{-2}. \tag{6.6b}$$

The values for r_p in Table 6.1 were calculated from Eq. (6.2b), which fulfills (6.6b), so the rest of the table will meet the Heisenberg constraint for frequency implied to factor-of-two precision by an oscillation observation. This consistency check seems to pass, at least well enough to permit flavor oscillations to be observable in expectancy.

To verify against the relativistic constraint of Eq. (4.5), we calculate the Table 6.1 tangential speed $v_\perp$ of a quirk feature in the neutrino rest frame as $v_\perp = r_p w_p$.

The combined quantal and relativistic results are entered in Table 6.2.

Table 6.2 Validation of the Table 6.1 data against relativistic and quantal constraints. All values based on w_p in the leftmost column.

Neutrino	Tabulated Quirk Frequency w_p (s^{-1})	Calculated Quirk Radius r_p (m)	Calculated Quirk Speed $v_\perp$ $(\mathrm{m \cdot s^{-1}})$	Relativistic Maximum Quirk Radius r_p (m)	Quantal Minimum Quirk Radius r_p (m)
Experimental	$5 \cdot 10^{13}$	$1.8 \cdot 10^{-14}$	0.9	$\sim 10^{-6}$	$\sim 7 \cdot 10^{-15}$
Atmospheric	$2.4 \cdot 10^{11}$	$2.6 \cdot 10^{-13}$	0.06	$\sim 10^{-4}$	$\sim 10^{-13}$
Solar	$3 \cdot 10^{5}$	$2.4 \cdot 10^{-10}$	$7 \cdot 10^{-5}$	$\sim 10^{2}$	$\sim 10^{-10}$

In table 6.2, which summarizes the basic consistency requirements, we also compute the maximum quirk radius possible at the given angular speed, using Eq. (6.7), as well as the minimum quirk radius possible fulfilling Eq. (6.2b).

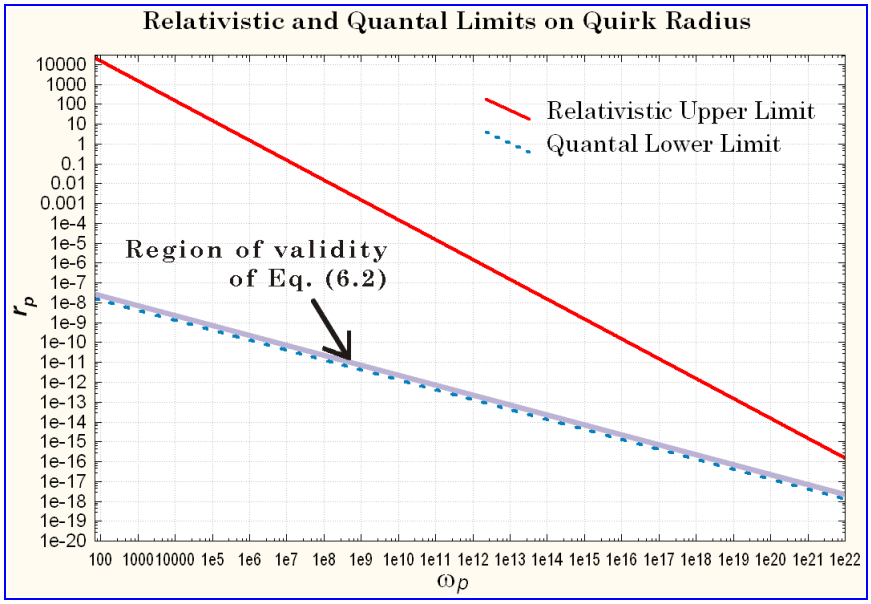

Figure 6.2. General physical limits on the hypothetical quirk radius r_p as a function of quirk frequency ω_p. The neutrino mass m = 1 eV/c^2, and the quirk structure n = 1 quantum of angular momentum.

The relation in Eq. (6.2b), which was shown to meet quantal constraints, sets a lower limit on r_p as a function of quirk frequency w_p. Solving Eq. (4.5) for $r \equiv r_p$, and replacing t_c with $1/(2\pi w_p)$, defines a relativistic upper limit on r_p. Both limits are plotted in Fig. 6.2.

So, it appears that the internal oscillation theory is consistent physically; the only worrisome issue would seem to be the huge values of the quirk structure radius r_p as estimated by the empirical data.

7. Exponentially Relaxing Compton Model Neutrino

In the light of Tables 6.1 and 6.2, we now examine how a model neutrino would behave under a reasonable guess at the law of quirk radius expansion. We abandon Table 6.1 except as a way of examining limits on neutrino behavior or of setting initial conditions on a model neutrino.

In this Section, we only are concerned with rate of change of the initial flavor F_1 as a function of distance; if the oscillation frequency is low enough at a distance at which oscillations have been observed, we assume all other features of a full theory of the neutrino can be developed. In the absence of any reliable appearance data as of mid-2002, we assume "optimistically" that all three main oscillation observations are not because of incoherent oscillations (*cf.* [1], 4.4.1), but rather allow deduction of a specific, stable, distance-dependent oscillation phase.

The SNO analysis [7] did not identify the flavor different from that at creation, so it can not help us here. We shall not test our model against data indicating quirk flavor order; we simply assume that the flavor order will become a measured value in the theory when more data become available.

7.1. Definition of the Model

The model is based on a process in which the neutrino's quirk structure is scaled to the Compton wavelength l_C of the particle. It may be viewed as the solution of a linear differential equation, possibly one with variable coefficients; the equation itself is not of any special interest, so we shall not be further concerned with it here. In this model, the quirk radius r_p is established at neutrino creation with some initial value r_{pi} and relaxes exponentially during propagation to a final value r_{pf}. The initial radius is defined by a parameter k_i as,

$$r_{pi} = k_i \, l_C = k_i hc/E \, ; \tag{7.1}$$

and, the final radius is defined by a second parameter k_f,

$$r_{pf} = k_f \, l_C = k_f hc/E \, ; \tag{7.2}$$

The model then is,

$$r_p(t) = (r_{pi} - r_{pf})e^{-t/T_{2p/3}} + r_{pf} \;=\; (k_i - k_f)\, l_C e^{-t/T_{2p/3}} + k_f \, l_C \;=\; \frac{hc}{E}\left((k_i - k_f)e^{-t/T_{2p/3}} + k_f\right), \tag{7.3}$$

in which the time constant $T_{2p/3}$ is the duration of the first of the three quirk phases during the first full cycle after neutrino creation.

We start by finding the time constant $T_{2p/3}$. We use (6.1) and (6.2a) and assume that at some angular frequency $< w >$ just after creation, r_p has grown during $T_{2p/3}$ from r_{pi} to e^{-1} of the total radial distance range, $|r_{pf} - r_{pi}|$:

$$T_{2p/3} = \frac{f}{3 < w >} = \frac{2p}{3 < w >} = \frac{2p}{3\left(\frac{2hn}{pm < r_p >^2}\right)} = \frac{p^2 m < r_p >^2}{3hn}; \tag{7.4a}$$

$$T_{2p/3} = \frac{p^2\left(e^{-1}(r_{pf} - r_{pi}) + r_{pi}\right)^2 m}{3hn} = \frac{p^2 hc^2\left(k_f + (e-1)k_i\right)^2 m}{3e^2 nE^2}. \tag{7.4b}$$

We need an expression for the quirk phase, $f(t_p)$, in order to plot the first dominant flavor F_1 as a function of proper time and thence distance of propagation. We start by finding an expression for the quirk frequency w, which we then may integrate to find f:

The model neutrino's oscillation radius has been defined in proper time by Eq. (7.3); combining that with (6.2a),

$$w_p(t_p) = \frac{12hn}{p\left((r_{pi} - r_{pf})e^{-t_p/T_{2p/3}} + r_{pf}\right)^2 m}; \text{ or,} \tag{7.5a}$$

$$w_p(t_p) = \frac{K_1}{\left(K_2 e^{K_3 t_p} + K_4\right)^2}, \text{ in which,} \tag{7.5b}$$

$K_1 = 12hn/(pm)$, $K_2 = r_{pi} - r_{pf}$, $K_3 = -1/T_{2p/3}$, and $K_4 = r_{pf}$.

Because by definition $w = df/dt$, we may use (7.5) to write an expression for the phase f elapsed after creation as in Table 6.1,

$$f(t_p) = \frac{12nh}{pm}\int_{t=0}^{t_p} dt \frac{1}{\left((r_{pi} - r_{pf})e^{-t_p/T_{2p/3}} + r_{pf}\right)^2}. \tag{7.6a}$$

Using the definitions for (7.5b) above, we may rewrite (7.6a) as,

$$f(t_p) = K_1\int_{t=0}^{t_p} dt \frac{1}{\left(K_2 e^{K_3 t} + K_4\right)^2}. \tag{7.6b}$$

The form of this integral yields to *MathCAD* or a table:

$$f(t_p) = \frac{K_1}{K_3 K_4}\left(\frac{1}{K_2 e^{K_3 t} + K_4} + \frac{K_3 t - \ln\left| K_2 e^{K_3 t} + K_4 \right|}{K_4} \right)_{t=0}^{t_p}; \tag{7.6c}$$

$$f(t_p) = \frac{K_1}{K_3 K_4}\left(\frac{K_3 t_p + \ln\left| K_2 + K_4 \right| - \ln\left| K_2 e^{K_3 t_p} + K_4 \right|}{K_4} + \frac{1}{K_2 e^{K_3 t_p} + K_4} - \frac{1}{K_2 + K_4} \right); \tag{7.6d}$$

$$f(t_p) = \frac{12hnT_{2p/3}}{pmr_{pf}}\left(\frac{\ln\left| (r_{pi} - r_{pf}) e^{-t_p / T_{2p/3}} + r_{pf} \right| - \ln r_{pi} + \dfrac{t_p}{T_{2p/3}}}{r_{pf}} + \frac{1}{r_{pi}} - \frac{1}{(r_{pi} - r_{pf}) e^{-t_p / T_{2p/3}} + r_{pf}} \right). \tag{7.6e}$$

Replacing $T_{2p/3}$ with the value of the time constant in (7.4b), simplifying, setting $m = n = 1$, and replacing r_{pf} and r_{pi} as in (7.1) and (7.2) above,

$$f(t_p) = \frac{4nE^2 t_p}{phc^2 {k_f}^2 m} + \frac{4p(k_f + (e-1)k_i)^2 E}{e^2 k_f}\left(\frac{\ln\left| (1 - k_f / k_i) e^{\frac{-3e^2 nE^2 t_p}{p^2 hc^2 (k_f + (e-1)k_i)^2 m}} + k_f / k_i \right|}{k_f} + \frac{1}{k_i} - \frac{1}{(k_i - k_f) e^{\frac{-3e^2 nE^2 t_p}{p^2 hc^2 (k_f + (e-1)k_i)^2 m}} + k_f} \right). \tag{7.6f}$$

7.2. Evaluation of the Model

Using Eq. (7.6f), we evaluate this model on the arbitrary assumption that the mass of the neutrino will be $m = 1 \text{ eV}/c^2$ and that the quirk structure will contain $n = 1$ quantum of angular momentum. Some experimentation shows it is possible to fit all three major neutrino problems by adjusting the two free parameters *k* of this model. Other values might be found to improve the result, but $k_i = 10^{-1/3}$ and $k_f = 10^{3.5}$ seem to do well enough. The result is in Fig. 7.1.

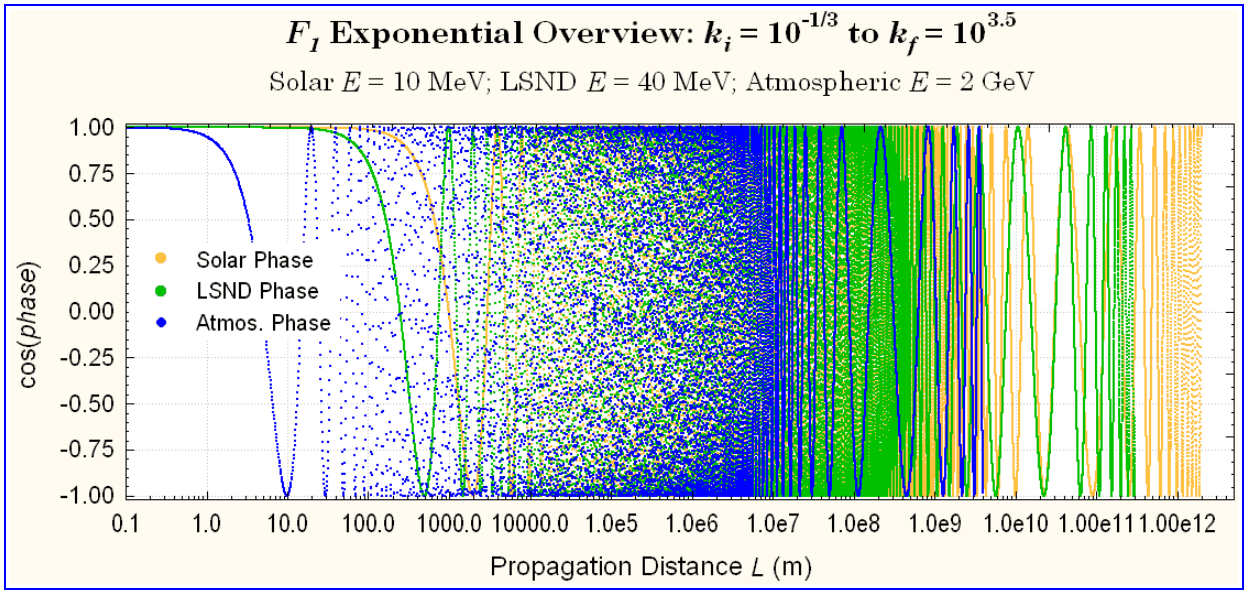

Figure 7.1. Overview of data fit of the exponentially-expanding model neutrino: Initial flavor state F_1, with $m = n = 1$. The plots for LSND and atmospheric energies are truncated on the right for visibility.

The logarithmic scale in Fig. 7.1 creates an interesting distortion of the actual process of quirk expansion: At short distances, the higher energy neutrino flavor states are compressed earliest by the log scale, because their frequencies are high. Toward the middle of the figure, the rate of quirk expansion begins to exceed the rate of scale compression, so the slowing of the visualized oscillation rate makes individual cycles appear again, as at short distances. Finally, at the largest distances, the quirk expansion is completed, and the log scale again compresses the cycles out of sight.

To verify the compliance with quantal and relativistic constraints, Fig. 7.2 may be compared with Fig. 6.2: The radius and frequency necessarily comply with quantal constraints because of the way they were defined; and, none of the energies plotted approaches a relativistic limit.

The fit of the exponentially-relaxing model in the individual problem domains is shown below. The overall fit is identical for all problem domains. This fit was

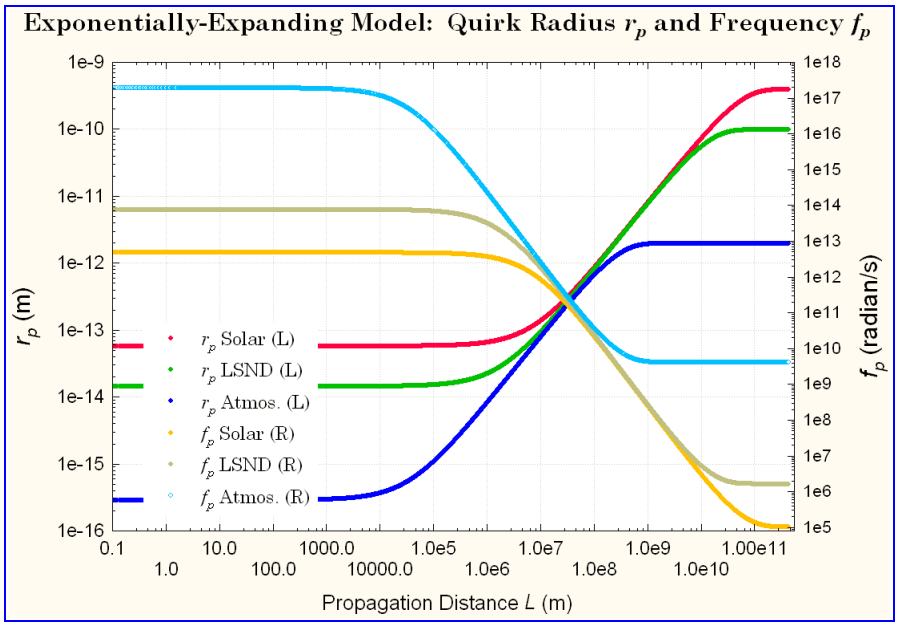

Figure 7.2. Quirk radius and frequency of the exponentially-expanding Compton neutrino: Parameters and neutrino energies were as in Fig. 7.1.

done by eye, and little attempt was made to optimize the parameter values. Because these models are only consistency tests, it was considered an adequate fit if the F_1 oscillation phase was not varying very rapidly at the propagation distance of interest.

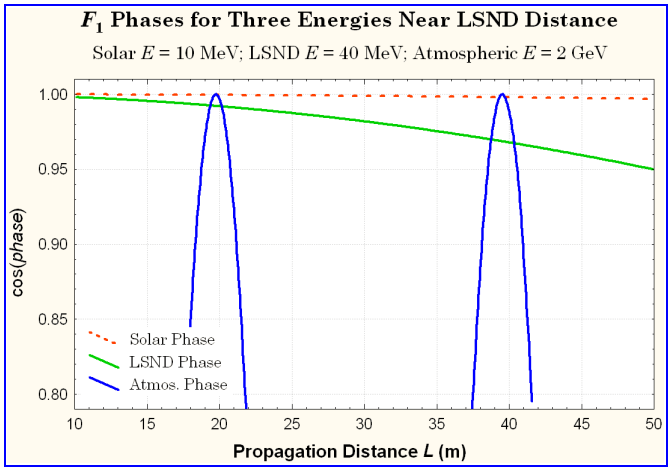

Figure 7.3. Exponentially-expanding Compton neutrino: LSND fit. Parameters as in Fig. 7.1.

The most difficult case for the usual superposition theory, LSND, was fit first; it was what required an initial quirk radius smaller than the Compton radius, namely $r_{pi} = 10^{-1/3}\, l_C$. The result is shown in Fig. 7.3. The 40 MeV neutrino ranges around a cosine value of 0.99 to 0.96 at distances comparable with the LSND experimental distances. There is easily enough of an effect to explain the reported LSND results.

Oscillations at the typical atmospheric distance, equal within a few hundred kilometers to the diameter of the Earth, are shown fit with the same parameter values in Fig. 7.4. In this case, the lower-energy neutrinos oscillate at very high frequencies, but at the atmospheric energy of 2 GeV, the phase is fairly constant. Looking at Fig. 7.2 for perspective, the three neutrinos at these distances are oscillating about at the same proper-time frequency; thus, the greater Lorentz time dilation for the atmospheric-energy neutrino is what causes it to show the lowest frequency in the lab frame.

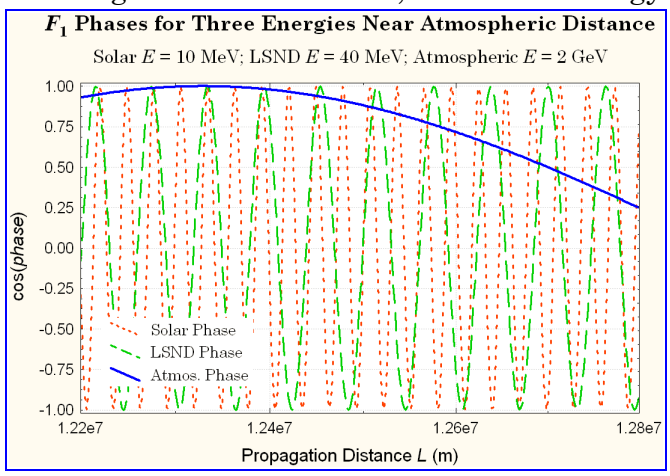

Figure 7.4. Exponentially-expanding Compton neutrino: Atmospheric fit. Parameters as in Fig. 7.1.

The Solar fit is shown in Fig. 7.5. At a propagation distance equal to the radius of the Earth's orbit, as may be seen from Fig. 7.2, all neutrinos have reached their final quirk radius values.

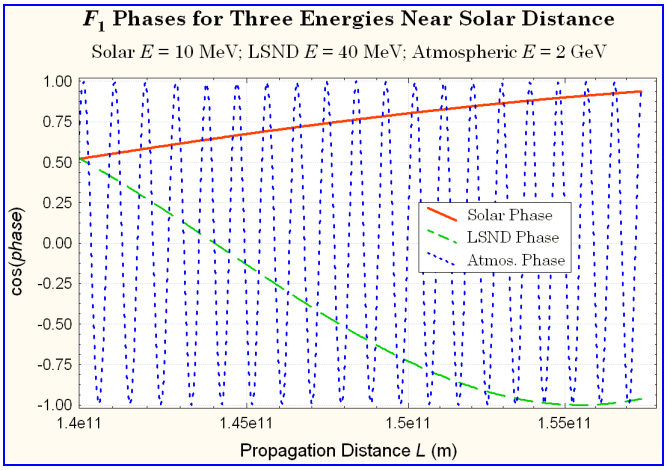

Figure 7.5. Exponentially-expanding Compton neutrino: Solar fit. Parameters as in Fig. 7.1.

Thus, at Solar distances, the larger quirk radii counter the smaller time dilations of the lower-energy neutrinos to give them relatively low oscillation frequencies.

It should be mentioned that the muon disappearance data for the KEK-to-Kamioka (K2K) experiment also would be explained adequately by the exponential-expansion fit in Fig. 7.1.

8. Conclusion

We have stated a set of assumptions leading to a totally new theory of neutrino flavor oscillations. It seems feasible physically, and a model based on the assumptions has been shown capable at least approximately of explaining the main neutrino problems suggesting oscillations.

In the proposed internal oscillation theory, distance (or neutrino proper time), and energy are measured values, as will be the order of flavor change. The quirk angular momentum (number of quanta) is fixed, given the quirk radius and neutrino mass. So, to predict a detected flavor from an initial flavor, this theory depends upon (*a*) the neutrino mass, (*b*) the initial quirk radius, r_{pi}, (*c*) the quirk radius expansion rule as given in Eq. (7.3), and (*d*) the final quirk radius, r_{pi}.

The advantage of this theory is internal consistency and conformance with all physical laws. The only worrisome feature is the apparent excessively large value of the final quirk radius in the neutrino rest frame: The final radius value seems too large to be aligned with intuitively appealing neutrino particle metrics such as the range of the weak force or the Compton wavelength.

The new theory requires an expansion rule and at most three free parameters, and implies no others, to fit the three data sets in Table 6.1. By comparison, the usual neutrino oscillation theory is based on a CKM-like flavor-mixing determined by propagation characteristics of a number of neutrino mass eigenstates. Ignoring CP violation, the usual theory typically would require three mixing angles and three mass differences, for a total of six or more free parameters, with perpetual ambiguity as to the number of mass eigenstates. In addition, the usual theory violates energy or momentum conservation and suffers several other discomforting inconsistencies described in [1].

Recent results [6] from the KARMEN collaboration showed no short-range oscillation at all, casting some empirical doubt on the LSND results. If KARMEN is confirmed by MiniBOONE, elimination of LSND from consideration would reduce the complexity of the usual oscillation theory by one or several free parameters, and it would reduce the need for quirk expansion in the proposed new theory. We look forward to further experimental developments in the rapidly changing neutrino landscape.

9. Afterthoughts

The tabulated values of r_p in Tables 6.1 and 6.2 exceed the assumed range of the weak force by various and quite large ratios; the values discussed in text *ca.* Eq. (4.15), and shown in Table 6.2, are truly huge. Viewing these as averaging artifacts, the initial radius has been scaled in the exponentially-expanding model neutrino to within a reasonable size range, but the final radius remains very large. This might be a problem for the proposed theory, even though the Lorentz-contracted values, *r*, in the lab frame would be within weak-force range.

Kiers & Tytgat [4] have explored long-range weak interactions by massless neutrino exchange. So, maybe the hypothetical quirk structure might actually reflect an arrangement of something massive in a weak potential, although beyond the range

of the weak force as determined by weak decay or scattering? The massless or relatively light exchange particles would be *neutrinissimos*?

In [2], it was proposed tentatively that perhaps a mass hierarchy for neutrinos might be maintained even in the face of flavor oscillations, if neutrino interactions took place in a two-stage process, first a *flavor set*, and then a *mass vertex*. This would imply a finite extent of the neutrino at least in the direction of propagation. Such an extended interval might be identified with the excessive sizes r_p of the quirk structure in the table above.

While in the current work we purposely ignore mass hierarchy in favor of simplicity, we are aware of the many unknowns about neutrinos; therefore, we suggest accepting the presumptively excessive values of r_p in the tables, at least until further evaluation of the present approach had been carried out.

10. References

1. J. M. Williams, "Some Problems with Neutrino Flavor Oscillation Theory", Posters and Commentary from a presentation at *SLAC 29th Summer Institute on Particle Physics*, 2001-08-15 and 2001-08-20. Available at the CERN web site (`http://weblib.cern.ch`) as `EXT-2002-042` (2002).

2. J. M. Williams, "Asymmetric Collision of Concepts: Why Eigenstates Alone are not Enough for Neutrino Flavor Oscillations", Posters and Commentary from a presentation at *SLAC 28th Summer Institute on Particle Physics*, ***arXiv***, `physics/0007078` (2001).

3. Y. Ahronov and B. Reznik, " 'Weighing' a Closed System and the Time-Energy Uncertainty Principle", *Physical Review Letters*, **84**(7), 1368 - 1370 (14 Feb. 2000 issue).

4. K. Kiers & M. H. G. Tytgat, "The neutrino ground state in a macroscopic electroweak potential", ***arXiv***, `hep-ph/9712463` (1997).

5. X. Calmet, H. Fritzsch, and Holtmannspoetter, "The anomalous magnetic moment of the muon and radiative lepton decays", ***arXiv***, `hep-ph/0103012` (2001).

6. B. Armbruster, et al (KARMEN Collaboration), "Upper limits for neutrino oscillations nubar_mu --> nubar_e from muon decay at rest", ***arXiv***, `hep-ph/0203021` (2002).

7. Q. R. Ahmad, et al (SNO Collaboration), "Direct Evidence for Neutrino Flavor Transformation from Neutral-Current Interactions in the Sudbury Neutrino Observatory", ***arXiv***, `nucl-ex/0204008` (2002).

11. Acknowledgments

Many thanks to Steven Yellin for enlightening discussions and suggestions. Stanley Brodsky and Lance Dixon encouraged early exploration of the assumptions on which the internal oscillation theory is based.

This document was composed in *Microsoft Word*. Graphs were created in *Statistica*, and some calculations were verified in *MathCAD*. Italicized words are used in trade by their owners.